Characterization of a Colloid Thruster Performing in the micro-Newton Thrust Range.

Manuel Gamero-Castaño & Vladimir Hruby
Busek Co. Inc.
11 Tech Circle
Natick, Massachusetts 01760
busek@busek.com
508-655-5565

IEPC-01-282

In this article we present results from the initial testing of a colloid thruster featuring 57 individual electrospray emitters. In particular, we measured the thrust and specific impulse associated with a propellant with an electrical conductivity of 0.50 S/m. With this propellant, the electrospray source could deliver thrust in the range 20/189 μN. Higher or lower thrust values can be obtained by either modifying the number of colloid emitters, or using a different propellant. The thruster, emitting droplets positively charged, was tested with a Field Emission electron source. We proved that this type of neutralizer provided the required charge neutrality of the spacecraft while consuming a power much smaller than that of the positive beam.

I. Introduction.

Propulsion systems operating in the micro-Newton range will enable the expected proliferation of nano and microspacecraft. On the other hand, there are a variety of scientific missions that require very precise thrusting capability in the micro-Newton range as well. A few examples of such missions are NASA's Laser Interferometer Space Antenna (LISA), Earth Science Experimental Mission 5 (EX-5), and Laser Interplanetary Ranging Experiment (LIRE). It is recognized that, among the different micropropulsion concepts, only Field Emission Electric Propulsion (FEEP) and Colloid thrusters might meet the most demanding propulsion requirements (especially those associated with thrust resolution, throatability and specific impulse).[1]

In this article we describe some performance parameters of a Colloid thruster prototype being currently developed by Busek Co. Inc. The main baseline requirement for the thruster is the capability of yielding thrust in the complete range 1/20 μN, with minimum resolution and specific impulse of 0.1 μN and 500 s. Furthermore, the thruster must incorporate its own neutralization scheme. The description of the overall thruster system is given in paper IEPC-01-281 presented in this Conference.[2] In this report we will focus on the characterization of its thrust and specific impulse, which were measured using the time of flight technique. We will also describe the interaction between the thruster and its Field Emission neutralizer. This research is being funded by the NASA JPL New Millennium Micro Newton Thruster Program, and a NASA GRC SBIR Colloid Thruster Program. The research on the carbon nanotube Field Emission cathode was sponsored by a BMDO SBIR program.

Presented as Paper IEPC-01-282 at the 27th International Electric Propulsion Conference, Pasadena, CA, 15-19 October, 2001

II. Results and Discussion.

Electrospray source and time of flight measurements

The colloid source is shown in Figure 1. It features 57 individual emitters (electrospray needles), and extractor and accelerator electrodes. The voltage

difference required to set the electrosprays (approximately 1800 V) is applied between emitters and extractor. The colloid beam can be further accelerated by increasing the potential of the extractor with respect to the accelerator. The diameter of the electrodes in Figure 1 is 53 mm. No especial considerations were taken to minimize the size of this source prototype. All components are made of 304 stainless steel, except the ceramic isolators placed between the electrodes. The propellant is fed through an external line inserted in the fitting observed in the bottom of Figure 1.

Figure 1 Photograph of the colloid source. The electrospray needles, and the extractor and accelerator electrodes can be seen in this view.

The initial testing of the colloid source was carried out with a solution of formamide with electrical conductivity K = 0.50 S/m. The source was placed in the experimental arrangement is shown in Figure 2. The thruster was mounted inside a 3¼" ID plexiglass tube, joint to a 3x4-feet cylindrical tank. The electrospray current was measured at a collector electrode installed inside the tank. A 10" diffusion pump backed by a mechanical pump could evacuate the system down to approximately 10^{-5} torr. The propellant was stored inside a glass reservoir outside the vacuum facility, and fed to the thruster through a fused silica capillary. The liquid flow rate could be varied by changing the pressure difference between glass reservoir and chamber.

We used time of flight diagnostics to measure the thrust and specific impulse associated with the beams. The electric connections and components needed to take these measurements are depicted in Figure 3. The charged beam exiting the thruster enters a drift section of null electric field, and eventually reaches a collector, connected to a fast electrometer. A screen of high porosity is biased negatively to eliminate spurious currents associated with secondary electrons emitted by highly energetic particles impinging in the collector. A high-speed, high-voltage switch is used to periodically short the needle voltage to ground. The falling time of the needle voltage is 0.8 μs, much smaller than the time of flight of the droplets. During the interval in which the needle is shorted, the electrospraying process is interrupted and a beam front moves toward the collector. The time of flight of this front can be measured by means of an oscilloscope connected to the electrometer output and triggered by the voltage signal of the electrospray needle. The response time of the electrometer is 2 μs, fast enough for measuring these electrospray beams. This arrangement is similar to that used by Gamero-Castaño & Hruby, where a more detailed description can be found.[3] We used two dedicated power supplies to run these experiments. The onset voltage (~1800 V) required to establish the electrosprays was set by a floating power supply, with HV leads connected to the needles and extractor electrodes. The beam of charged particles can be further accelerated by raising the potential of the extractor, V_E, with respect the laboratory ground, which was accomplished with a second power supply. The acceleration voltage of the beam is then $V_{ON}+V_E$ minus a voltage loss associated with the formation of the cone-jet. This voltage loss can be measured using the stopping potential technique. We have measured previously this voltage loss for a variety of formamide solutions. For K = 0.50 S/m, the voltage loss is approximately 200V.[3]

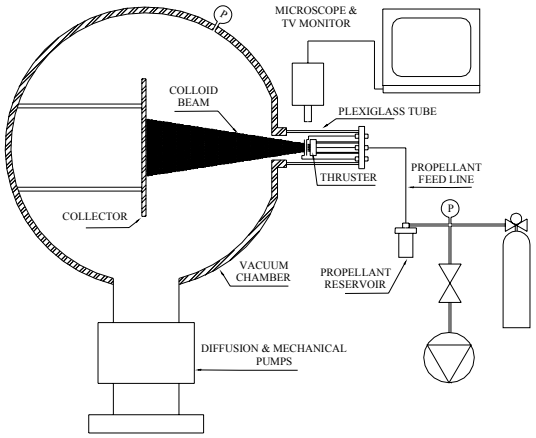

Figure 2 Experimental arrangement employed to test the thruster.

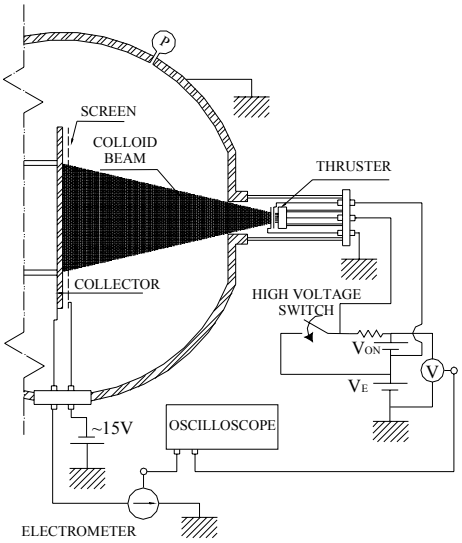

Figure 3 Schematics of the time of flight setup.

Figure 4 shows images of the colloid emitters when the electrosprays are turned on. The photograph on the left contains a single needle aligned with a facing opening. This opening is a hole perforated on the extractor, and allows the passage of the electrospray. The conical shape observed at the tip of the needle is the electrospray cone-jet. A few needles operating simultaneously are featured in the right photograph.

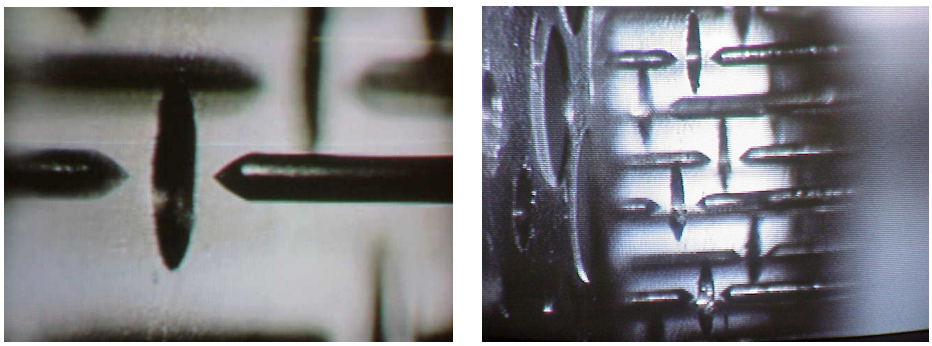

Figure 4 Photographs of the colloid emitters while operating.

Figure 5 contains the time of flight waves of several electrosprays. The onset and extractor voltages are kept fixed, V_{ON} = 1791 V and V_E = 2000 V respectively. Thus, the acceleration voltage of the beams is approximately V_A = 3600 V. Different curves are associated with different flow rates, which are controlled by varying the pressure inside the glass reservoir. We also plot the evolution of the voltage difference between needles and extractor, which is controlled with the high voltage switch. The thrust and mass flow rate of each beam are computed by integrating its time of flight spectrum:

$$T = \frac{2V_A}{L}\int_0^\infty t\ I'\ dt \qquad [1]$$

$$\dot{m} = \frac{2V_A}{L^2}\int_0^\infty t^2\ I'\ dt \qquad [2]$$

where L is the distance between needle electrode and collector plate. Specific impulse and thrusting efficiency η are obtained from the usual definitions:

$$I_{sp} = \frac{T}{\dot{m}g}, \quad \eta = \frac{T^2}{2\dot{m}(V_{ON} + V_E)I} \qquad [3,4]$$

The pairs of points thrust versus mass flow rate, and specific impulse versus mass flow rate, associated with these beams and others with lower acceleration voltages are plotted in Figure 6 and Figure 7. Additional parameters such as the beam current, Isp and thrusting efficiency are collected in Table 1. Note that the range of measured thrust (20-189 μN) is above that specified by the thruster baseline (1-20 μN). This is motivated by the use of a formamide solution with a conductivity relatively low. If a solution with K~1.5 S/m were used instead, the thrust delivered would fall on the desired range. This low conductivity also penalizes the specific impulse, in every case lower than the baseline value of 500 s. Alternatively, and if the specific impulse requirement were removed, the 0.5 S/m solution could perform in the desired thrust range by reducing the number of emitters of the thruster. In any case, these data prove that thrust ratios as large as 8 can be obtained with this colloid thruster. This conclusion is independent of the conductivity of the propellant.

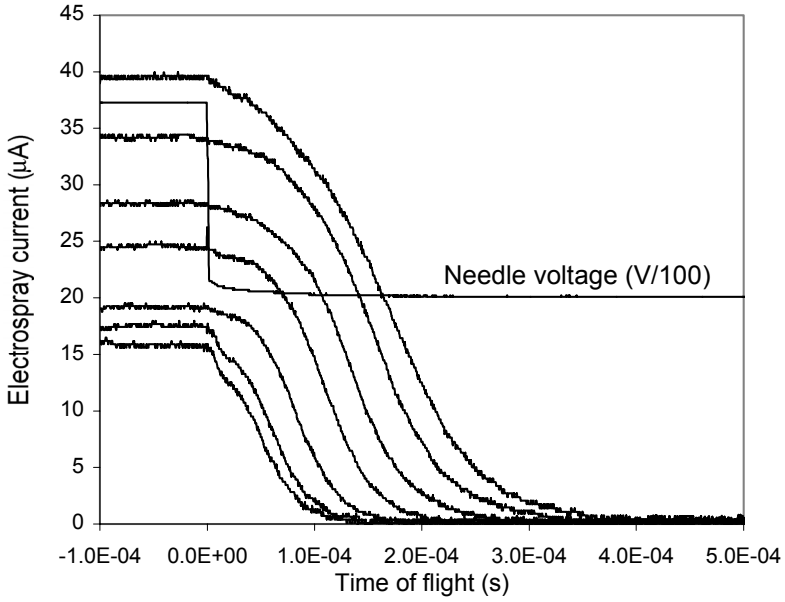

Figure 5 Time of flight curves. The onset voltage is 1791 V, and the electric potential of the needle electrode is 3791 V.

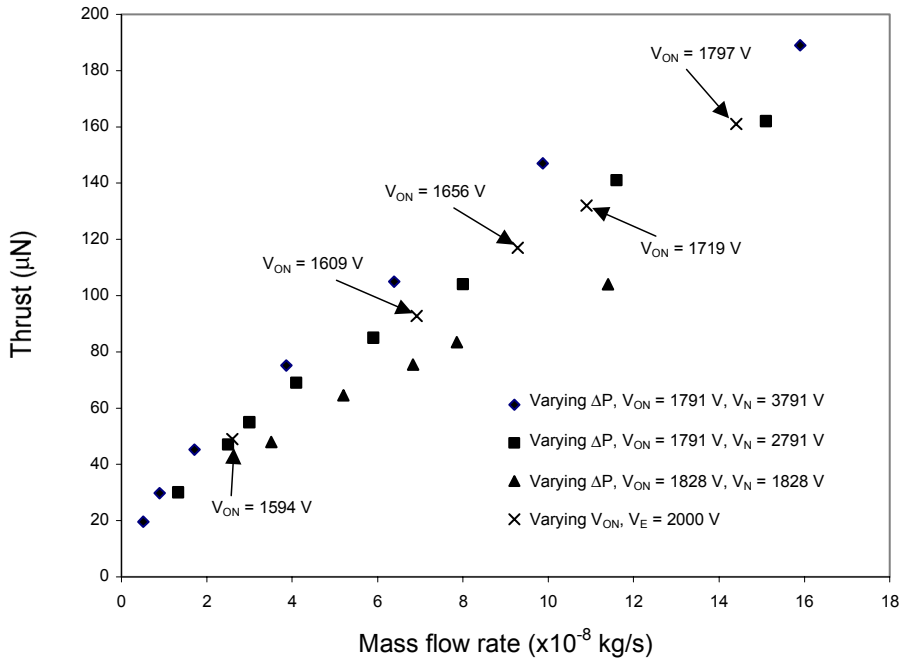

Figure 6 Thrust versus mass flow rate for the electrospray beams of a formamide solution K =0.50 S/m. The figure collect data for both "pressure controlled $\dot{m}$" (three first series, taken at different acceleration voltages), and "voltage controlled $\dot{m}$" (last data series) strategies.

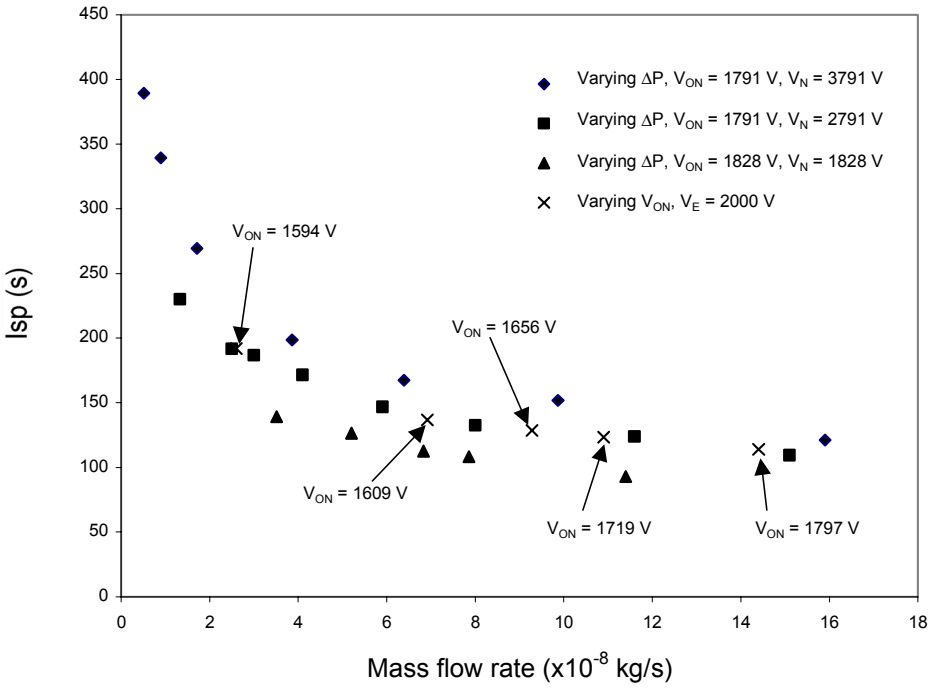

Figure 7 Specific impulse versus mass flow rate for the electrospray beams of a formamide solution K =0.50 S/m. The figure collect data for both "pressure controlled $\dot{m}$" (three first series, taken at different acceleration voltages), and "voltage controlled $\dot{m}$" (last data series) strategies.

The liquid flow rate can be also modified by varying the onset voltage. In this case, the electrostatic pressure on the surface of the cone-jet has to be comparable to the pressure drop along the electrospaying needles. It turns out that this strategy for flow control is possible for the combination of our electrospray needles and formamide solution. The time of flight spectra shown in Figure 8 were obtained using this method to control the electrospray flow rate. The extractor voltage is kept constant, V_E = 2000 V, while V_{ON} is varied between 1594 V and 1797 V. The pressure inside the thruster reservoir is brought to zero by evacuating the glass container where the propellant is stored. The thrust and specific impulse of these sprays are plotted in Figure 6 and Figure 7. Interestingly enough, a thrust throatability of almost 4 is achievable by simply varying V_{ON}. Notice that a larger thrust range could be obtained by modifying the extractor voltage.

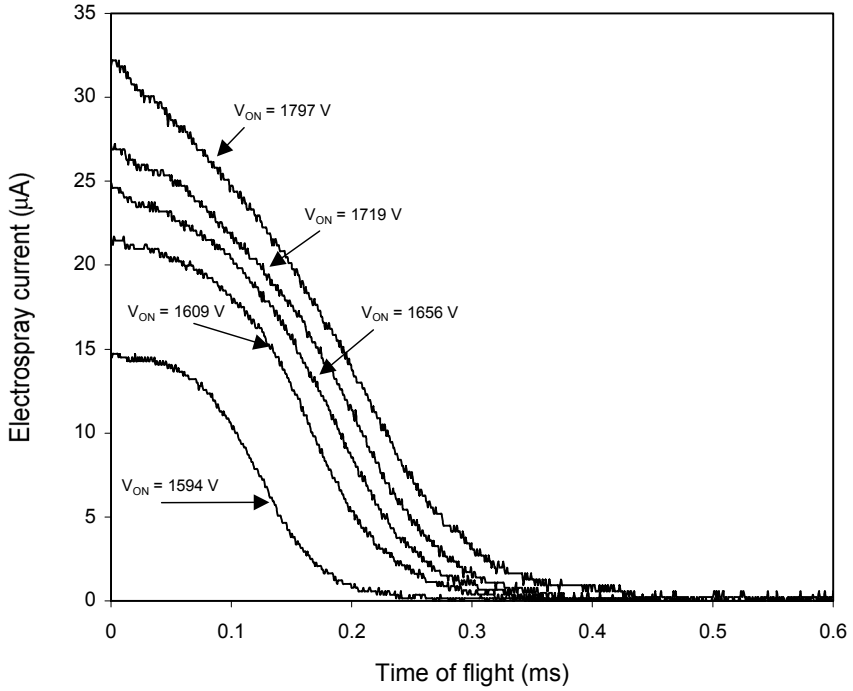

Figure 8 Time of flight curves. The onset voltage is varied, while keeping the pressure in propellant reservoir constant an equal to 0. The extractor voltage is set to 2000 V.

Cathode performance and neutralization of the colloid beam

The electron source used to neutralize the exiting beam of positive droplets is based on the remarkable field emission properties of carbon nanotubes.[4] The main parts of the electron source are a cathode with a substrate of carbon nanotubes and a facing gate. A better description can be found in reference [2]. The performance of this electron source was studied in the experimental arrangement schematized in Figure 9. The potential of the cathode is taken as the reference value, while the voltages of both gate and anode can be varied and measured. Also the electric currents released by the cathode and entering the gate and anode can be monitored and recorded by a data acquisition system. In the first set of data shown in Figure 10 we plot the electric currents at each electrode as a function of the voltage of the anode. In each plot the gate voltage is kept fixed. Notice the noisy aspect of the spectra, which is a characteristic of the carbon nanotube's electron emission process. The sum of gate and anode currents is equal to the cathode current, which indicates that ionization of gas molecules between the gate and anode is unimportant. More interesting is the evolution of the current collected at the gate and anode. The first remarkable observation is that,

regardless of the value of the current emitted by the cathode, the anode must be +29 V biased in order to start receiving electron current (see Figure 11). It could have been expected a bias value of +5 V (the electron work function for carbon) instead. The larger value of 29 V seems to be due to the effect of space charge between the gate and the anode. When the voltage of the anode is further increased, the electron current collected at this electrode augments, while the current intercepted by the gate diminishes. This trend is also governed by space charge in the region between gate and anode. Once the voltage of the anode is approximately 100 V the gate and anode currents stabilize and become comparable, i.e. the transmittance of the electron source is ~50%. When the voltage of the anode is larger than that of the gate, the transmittance increases and it actually exceeds the porosity of the gate (62%). In Figure 12 we plot similar spectra, in which the anode's potential is kept fix while we vary the voltage of the gate. Once a given onset gate voltage is exceeded (~250 V in Figure 12, this value depends on the spacing between cathode and gate), the electron current emitted by the cathode increases exponentially with the applied electric field, which is a characteristic feature of all field emission phenomena.

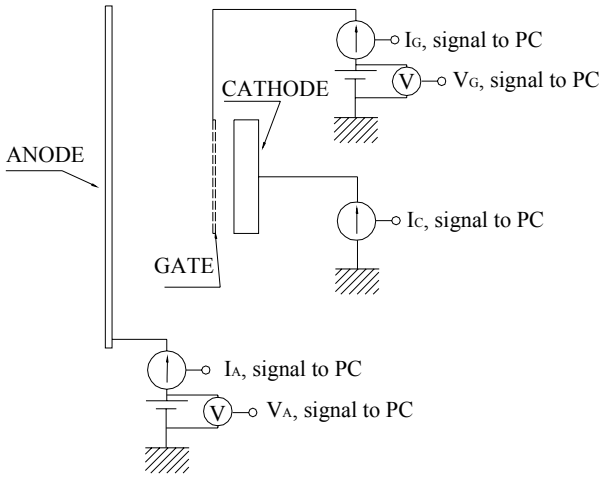

Figure 9 Schematics of the arrangement used to study the emission properties of the electron source.

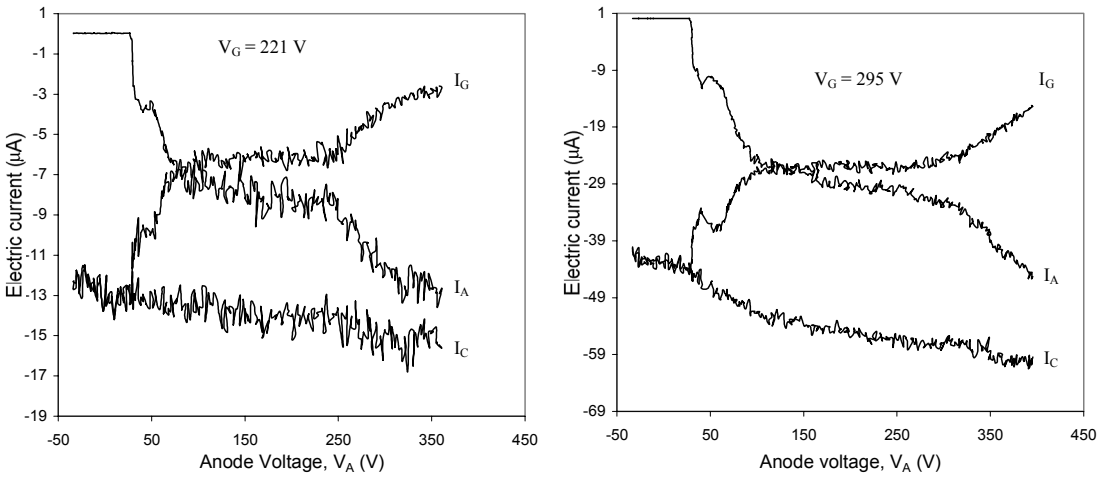

Figure 10 Electronic current measured at cathode, anode and gate as a function of anode voltage

Table 1 Experimental parameters associated with the colloid beams investigated. We tabulate the onset voltage, the potential of the needle electrode, the mass flow rate and thrust of the beams (both measured with the time of flight technique), the beam current, specific impulse and thrust efficiency.

V_{ON} (V)	V_N (V)	$\dot{m}$ ($x10^{-8}$ kg/s)	T (μN)	I (μA)	Isp (s)	η (%)
1791	3791	15.9	189	39.6	121	75
1791	3791	9.87	147	34.1	152	85
1791	3791	6.39	105	28.2	167	81
1791	3791	3.86	75	24.4	198	79
1791	3791	1.71	45	19.0	269	83
1791	3791	0.89	30	17.6	339	74
1791	3791	0.51	20	14.0	389	70
1791	2781	15.1	162	40.9	109	76
1791	2781	11.7	141	37.7	124	81
1791	2781	8.00	104	31.0	132	78
1791	2781	5.90	85	28.4	147	77
1791	2781	4.10	69	25.3	171	82
1791	2781	3.00	55	21.9	187	83
1791	2781	2.50	47	20.0	192	79
1791	2781	1.33	30	16.1	230	76
1828	1828	11.4	104	36.1	93	72
1828	1828	7.86	83	31.5	108	77
1828	1828	6.83	75	30.1	113	75
1828	1828	5.20	64	27.7	126	79
1828	1828	3.51	48	22.8	139	78
1797	3797	14.4	161	32.1	114	74
1719	3719	10.9	132	27.2	123	79
1656	3656	9.28	117	24.5	128	82
1609	3609	6.92	93	21.5	137	80
1594	3594	2.60	49	15.1	192	85

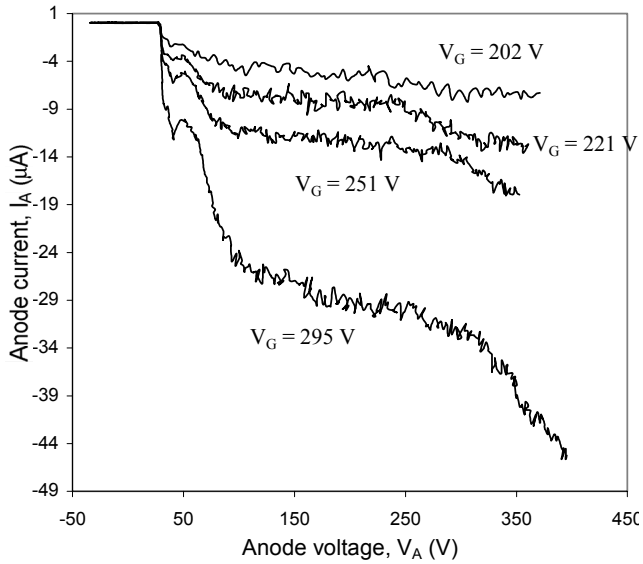

Figure 11 Electronic current measured at anode as a function of anode voltage for several gate voltages.

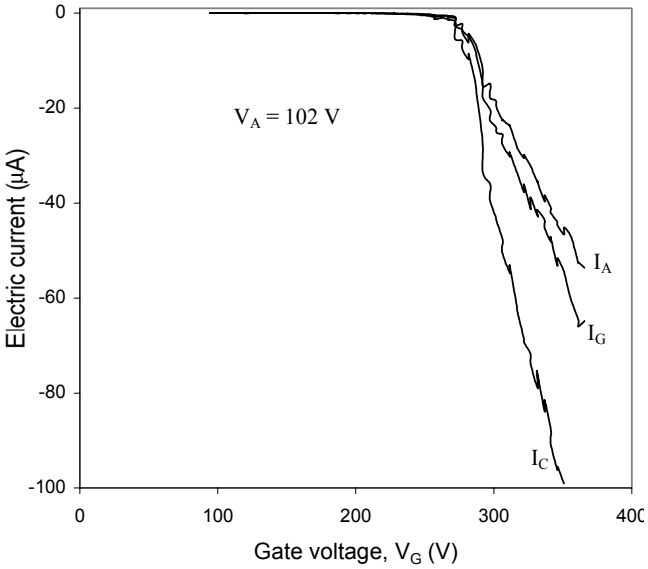

Figure 12 Electronic current measured at cathode, anode and gate as a function of gate voltage

We have studied the ability of this field emission cathode for neutralizing the colloid beam using the experimental arrangement shown in Figure 13. Notice that the cathode was placed inside the larger tank of the vacuum system, approximately 5 cm downstream the accelerator electrode. We could not place the cathode closer to the accelerator because there was no space available inside the plexiglass tube. However, this should not make any difference because the background pressure is the same in either point. Indeed, if there were to be any problem related to the impinging of liquid droplets on the cathode, this problem would augment close to the collector plate. Following with the description of Figure 13, we point out that the PPU circuit designed for the thruster prototype[2] was used to power the thruster and the gate of the electron source, and to turn on/off the electron source depending on whether neutralization is required or not. The first strategy employed in the neutralization of the colloid beam is better understood by looking at the circuit designed to turn on the electron source, which is shown in Figure 14a. It is basically a Schmitt trigger comparator

driving a high voltage EMCO DC-DC converter that powers the gate of the electron source. While the voltage difference between lab ground and cathode ground is smaller than 6.9 V, the output of the comparator is 0 V, the mosfet transistor is in non conduction mode and the voltage out of the EMCO DC-DC converter is 0 V. On the other hand, when the voltage difference between lab ground and cathode ground overcomes the barrier of 6.9 V, the output of the comparator is 6 V, the mosfet transistor is in conduction mode and the voltage out of the converter is approximately 600 V. This value promotes the emission of electrons from the cathode, neutralizing the beam and "discharging the cathode ground" (actually the electron current delivered by the source at 600 V gate voltage is many times larger the electrospray current). Ideally, because the comparator circuit has only one triggering level (6.9 V), the EMCO converter would turn on/off at a very large frequency. In reality the response time of the EMCO converter is a few tenths of a second, so its output self adjust as to operate continuously, in such way that the current emitted by the electron source neutralizes exactly the colloid beam. The experimental results obtained using this control strategy are shown in Figure 15. Here we plot the electrospray current (measured at the HV cable powering the needle electrode), the electron current emitted by the cathode, and the voltage difference between cathode ground and lab ground (V2-V3), as a function of time. Initially the cathode and lab grounds are connected (V2-V3 = 0 V) and an electrospray beam of I = 17 μA is emitted. Then, at a given time (t = 0 s), the connection is eliminated and both voltage references are isolated from each other. From this point on the cathode ground charges negatively with respect the lab ground and V2-V3 decreases. The slope of this signal is 0.22 V/s, very much coinciding with the ratio between the average of the electrospray current and the nominal value of the capacitor placed between lab and cathode grounds, 0.25 V/s (17/68 μA/μF). When V2-V3 reaches the value of –6.9 V, the EMCO converter is turned on and the cathode ejects an average current of 34 μA, sufficient to neutralize the exiting beam (approximately 50% of the electronic current is intercepted by the gate of the electron source). Clearly, once electron current is emitted the voltage difference between cathode and lab grounds remains constant.

Pulsing the electron source is an alternative strategy for achieving charge neutralization. In this case, the resistor network controlling the triggering state of the comparator is replaced by the circuit shown in Figure 14b. Elementary analysis shows that the comparator output will swing from 0 V to 6 V when V2-V3 reaches the value of –7.3 V, and it remains at 6 V until V2-V3 decreases to –6.8 V. We show in Figure 16 the actual evolution of the cathode current and V2-V3 when this control strategy is employed. Notice the initial ramping of the signal V2-V3, the onset of electron emission in the form of a current pulse when V2-V3 reaches for the first time the value of –7.3 V, and the periodic evolution of electron current pulses and the signal V2-V3 from this time on.

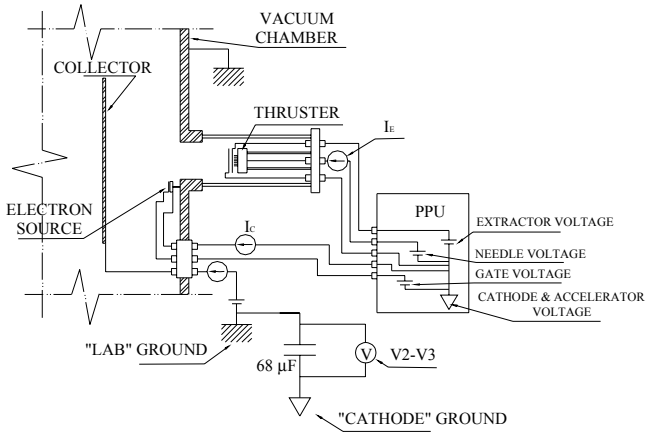

Figure 13 Schematics of the experimental setup used to test the neutralization of the electrospray beam.

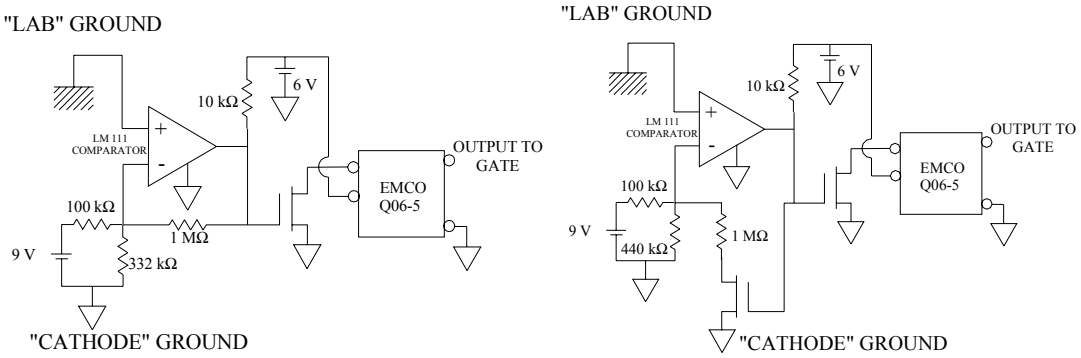

Figure 14a,b Diagrams of the circuits used to turn on/off the electron source in order to neutralize the colloid beam. The first circuit provides continuous neutralization. The second can be used for pulsing the operation of the electron source.

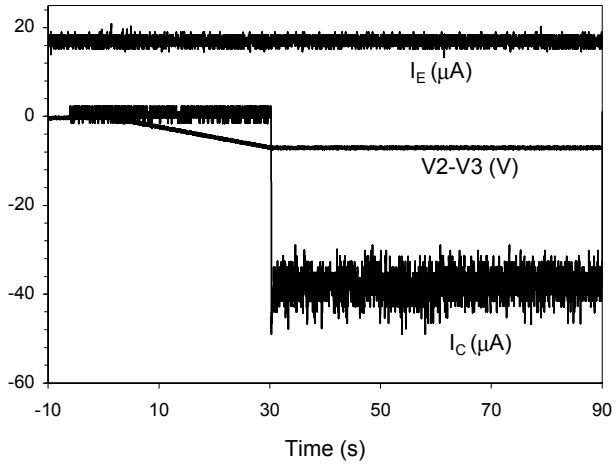

Figure 15 Evolution of the voltage difference between "cathode" and "lab" grounds, and the electrospray and cathode currents as a function time. Continuous electron emission is used to neutralize the electrospray beam.

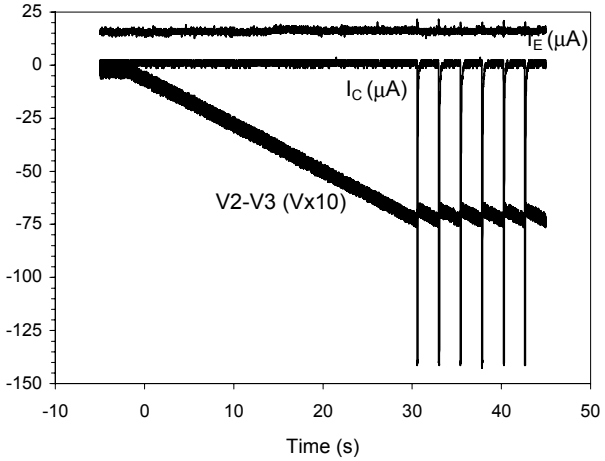

Figure 16 Evolution of the voltage difference between "cathode" and "lab" grounds, and the electrospray and cathode currents as a function time. The electron source is pulsed to achieve "neutralization" of the electrospray beam.

Finally, notice that these results do not prove that the space charge of the beam exiting the thruster is null. They simply indicate that the positive (colloids) and negative (electrons) currents emitted by the thruster are equal. The distance at which the beam is effectively neutralized will depend upon several factors such as the relative orientation between the electrospray and electron sources, and the energy of the electrons.

III. Conclusions

We demonstrated that the colloid source could deliver thrust in the range 20-189 μN with a maximum specific impulse of 389 s. In order to reach the baseline values (1-20 μN and 500 s), a more conducting propellant (~1.5 S/m) will be tested in the near future. This will increase the specific impulse above 500 s and lower the thrust associated with each single emitter, as proved in reference [3]. We also plan to do thrust measurements with a torsional balance developed in house, and which has a demonstrated resolution of 0.01 μN at frequencies lower than 0.5 Hz.[5] Two different ways of feeding the required propellant flow rate to the colloid emitters were studied. In the first one the liquid was driven by pressurization of the propellant tank. The second strategy involved varying the electrostatic pressure at the tip of the electrospray emitters.

A carbon nanotube Field Emission cathode was characterized and tested with the colloid source. We proved that this cathode could deliver the electronic current required to neutralize the beam. Its easy operation and low power consumption make this cathode an ideal neutralization device for electric micropropulsion thrusters. We plan to study in more detail the interaction between the colloid and electronic beam. In particular, we will characterize the conditions required for a fast reduction of the space charge of the colloid beam

Acknowledgements

Three programs contributed to the work presented herein including the NASA JPL New Millennium Micro Newton Thruster Program led by Dr. J. Blandino and Dr. W. Folkner, NASA GRC SBIR Colloid Thruster Program led by Dr. J. Sovey and Carbon Nanotube Field Emission Cathode Program led by Mr. C. Sarmiento of NASA GRC and sponsored by BMDO SBIR office under Mr. J. Bond. The authors would like to thank all of them for the opportunity to work on this exciting technology.

1 J. Reichbach, R. Sedwick & M. Martínez-Sánchez. "Micropropulsion System Selection for Precision Formation-Flying Satellites". Paper AIAA-2001-3646, 37th Joint Propulsion Conference, Salt Lake City, UT (2001).

2 V. Hruby, M. Gamero-Castaño, P. Falkos & S. Shenoy. "Micro Newton Colloid Thruster System Development". Paper IEPC-01-281, *27th International Electric Propulsion Conference*, Pasadena, CA, October 2001.

3 M. Gamero-Castaño & V. Hruby. "Electrospray as a Source of Nanoparticles for Efficient Colloid Thrusters", J. of Propulsion and Power 17, 977-987 (2001). Also as AIAA Paper 2000-3265 , 36th Joint Propulsion Conference, Huntsville, AL (2000)

4 W.A de Heer et al. A Carbon Nanotube Field-Emission Electron Source. Science, 270, 1179, (1995)

5 M. Gamero-Castaño & V. Hruby, "A Torsional Balance that Resolves sub-micro-Newton Forces". Paper IEPC-01-235, *27th International Electric Propulsion Conference*, Pasadena, CA, October 2001.